

Supplementary Materials

Dimitrova et al. Preterm birth alters the development of cortical microstructure and morphology at term-equivalent age.

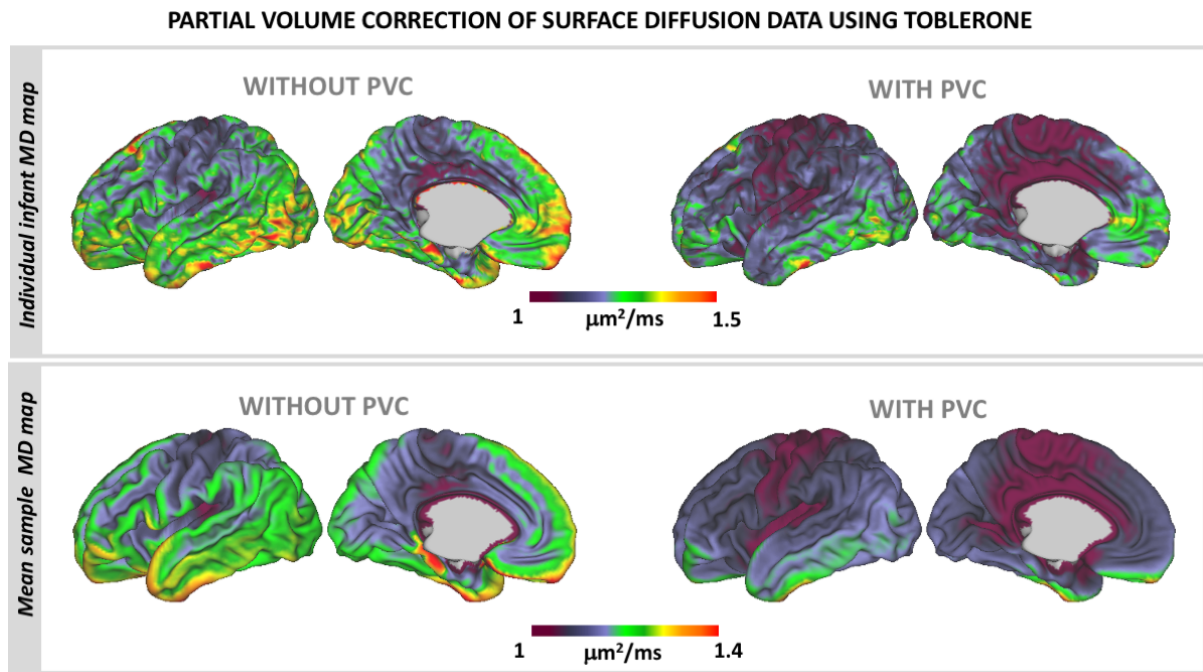
Partial volume correction

Despite achieving 1.5 mm isotropic voxel resolution in the dHCP, the dMRI data voxel resolution remains larger than the estimated ~1.1mm neonatal cortical thickness (Makropoulos et al. 2018). We applied partial volume correction (PVC) by estimating partial voluming on a voxel level using Toblerone (Kirk et al. 2020). This resulted in 3 tissue probability maps (GM, WM, CSF). Voxels with cortical probability < 5% were masked out from the projection to the surface. *Supplementary Figure 1* shows the difference between MD surface with and without PVC for a single infant (upper panel) and mean group average for the term-born sample (lower panel).

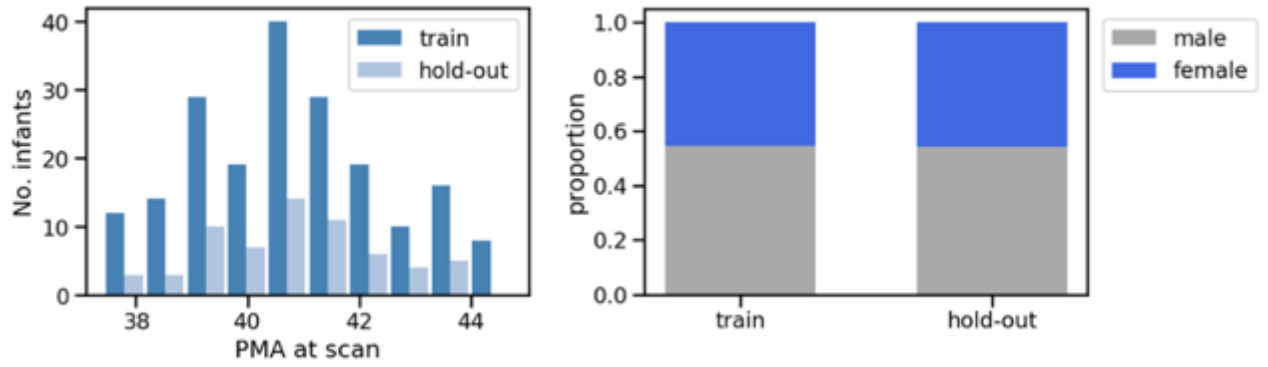
Quality control for dMRI and sMRI data

The initial sample consisted of 400 term and 109 preterm infants scanned at TEA with acquired dMRI and structural MRI (sMRI) data. We used a two-stage quality control (QC). Exclusion of subjects is broken down in *Supplementary Table 1*. Initial QC was performed in volume space and examined the success of the sMRI and dMRI preprocessing pipelines. QC of the sMRI data included visual examination of motion corrected T₂-weighted images following a scoring method described in (Makropoulos et al. 2018). For dMRI data, nominal metrics of the total amount of motion were estimated from the output translation and rotation trajectories of every subject. These translation and rotation metrics were respectively defined as the root sum of squares of the forward difference of the translation parameters (in mm) and the rotation parameters represented in Lie algebra (Claraco, 2018). When combined, they relate to the total length of the subject's motion trajectory during the entire dMRI sequence. A summary motion QC metric was quantified for every infant following the procedure described in (Christiaens et al. 2021), and data of insufficient quality were excluded (QC score > 3.5). Further visual assessment confirmed the success of preprocessing, alignment to T₂-weighted native space and ensured that all brain data were within the field of view (i.e., dMRI data where part of the cortex was cropped due to the infant moving out of the field of view were excluded). The second QC was performed in surface space and involved visual examination of individual surfaces ensuring successful projection, no gross misalignment to the 40-week dHCP surface template or cropped cortex not noted in volume space. Seventeen term infants were excluded from the term sample due to incidental findings. The final sample consisted of 259 term and 76 preterm infants.

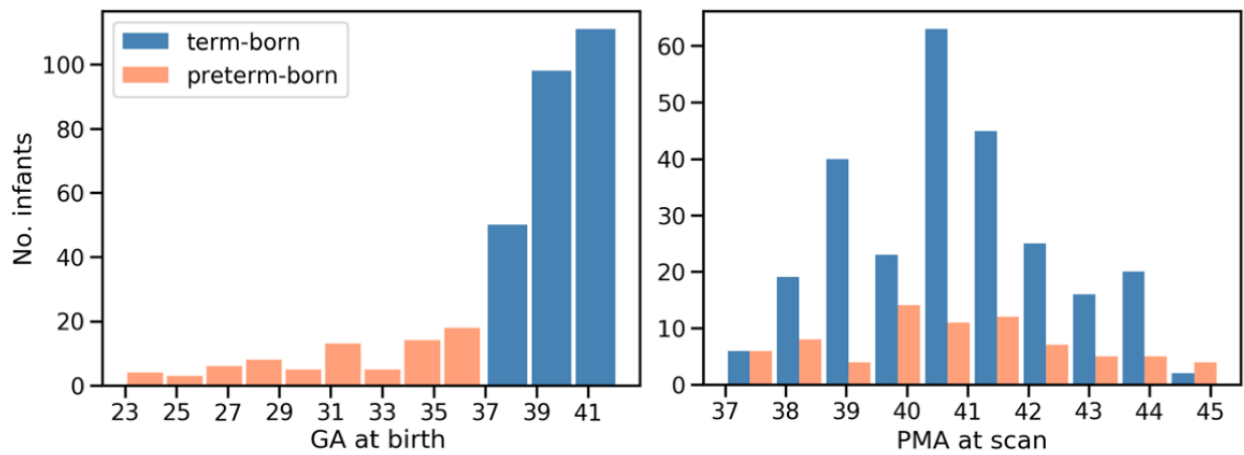
Supplementary Figures



Supplementary Figure 1. Partial volume correction (PVC). Individual infant Mean Diffusivity (MD) surface map without and with PVC (upper panel). Average Mean Diffusivity map without and with PVC for the term-born sample (lower panel).



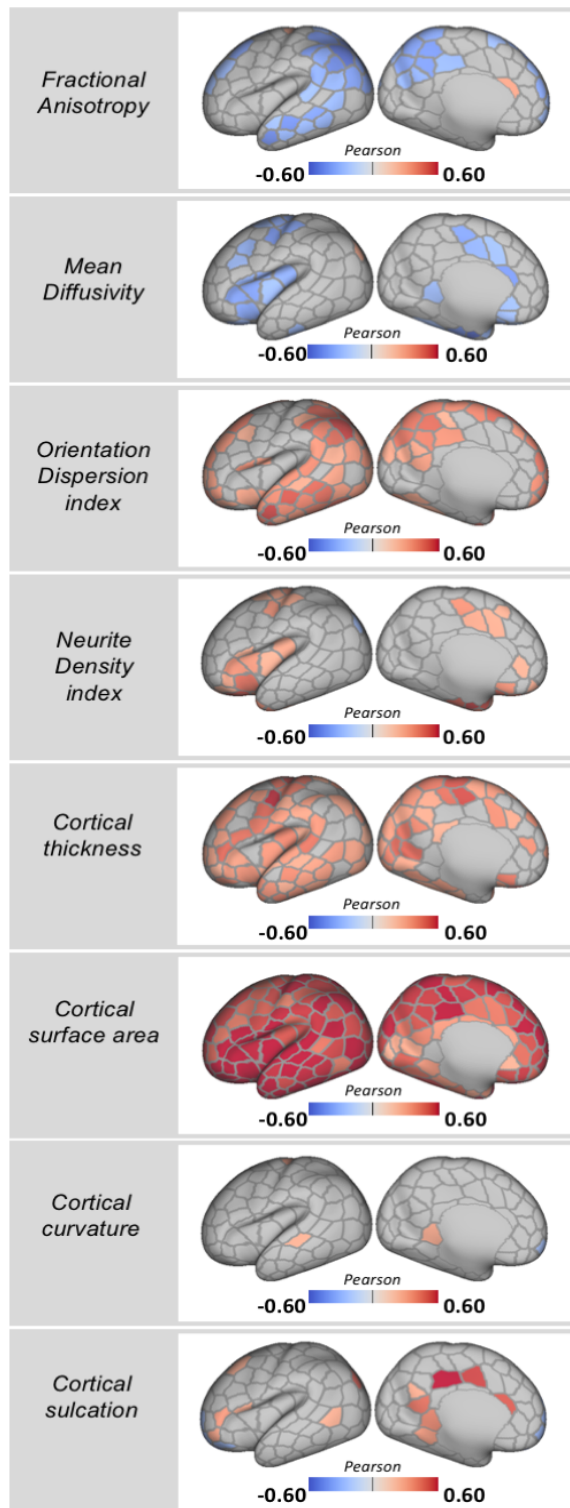
Supplementary Figure 2. Distribution of PMA at scan and sex proportion between train and hold-out term-born sample split used in the RF and GPR modelling.



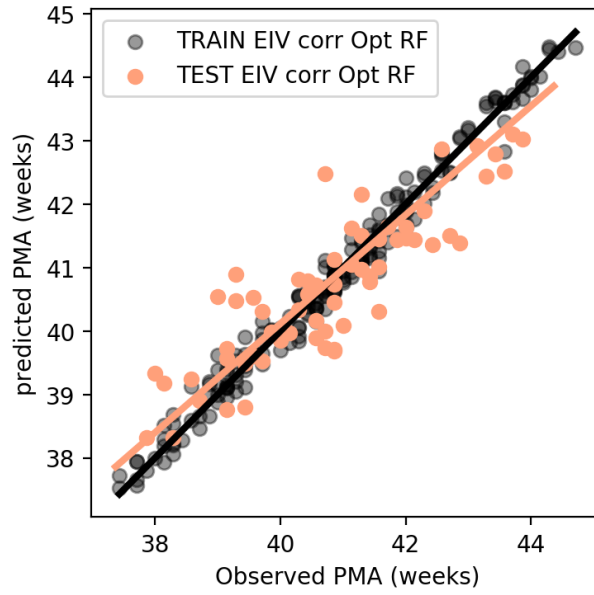
Supplementary Figure 3. Distribution of GA at birth and PMA at scan in the term-born and preterm samples.

CORRELATION WITH PMA AT SCAN

LEFT HEMISPHERE

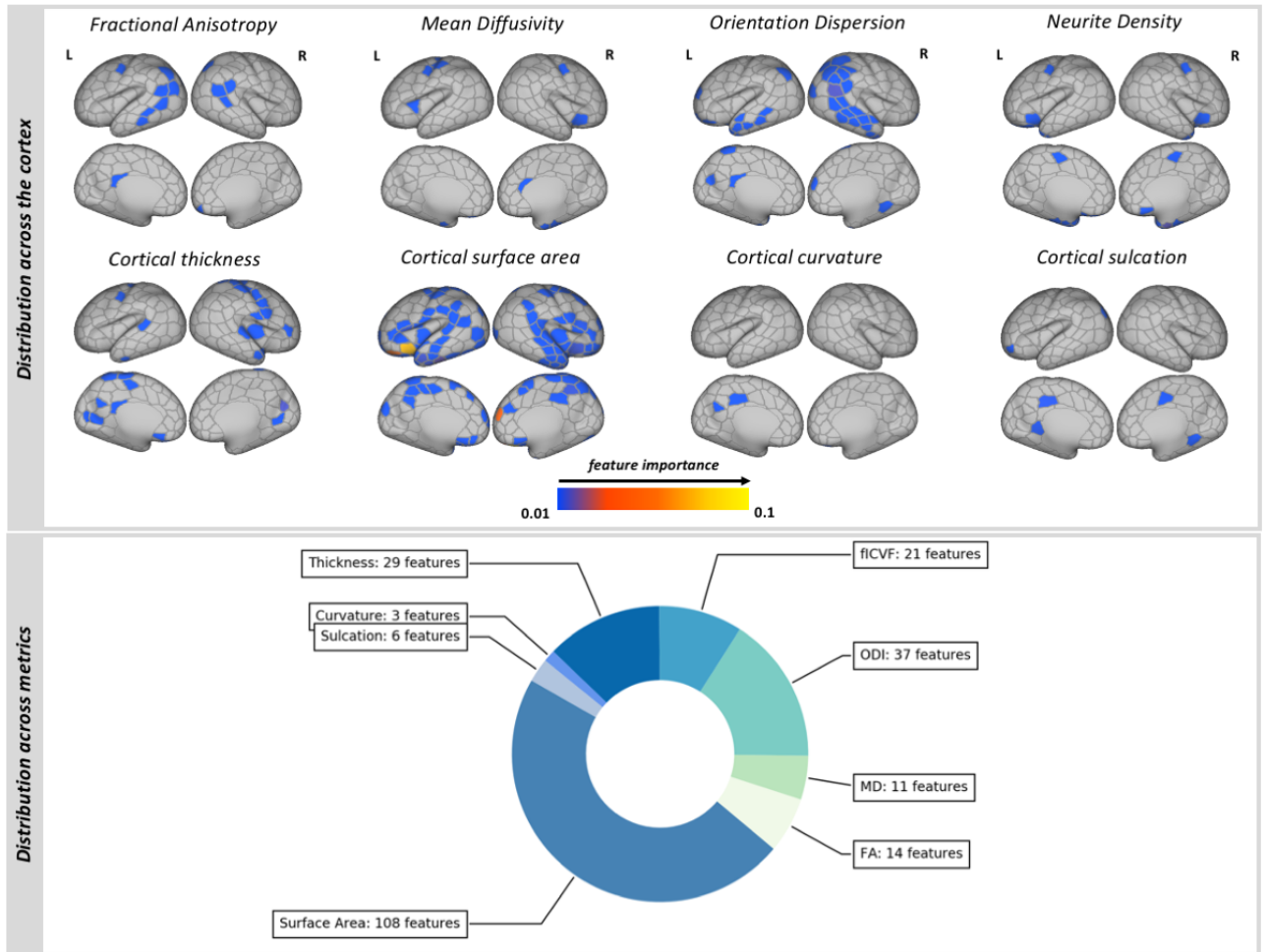


Supplementary Figure 4. Rapid regionally specific cortical micro- and macrostructure development in term-born infants during the neonatal period. Pearson's correlation coefficient for all parcels in the left hemisphere showing significant ($p_{\text{mcfwc}} < 0.05$) positive (red) or negative (blue) association with age (PMA at scan).



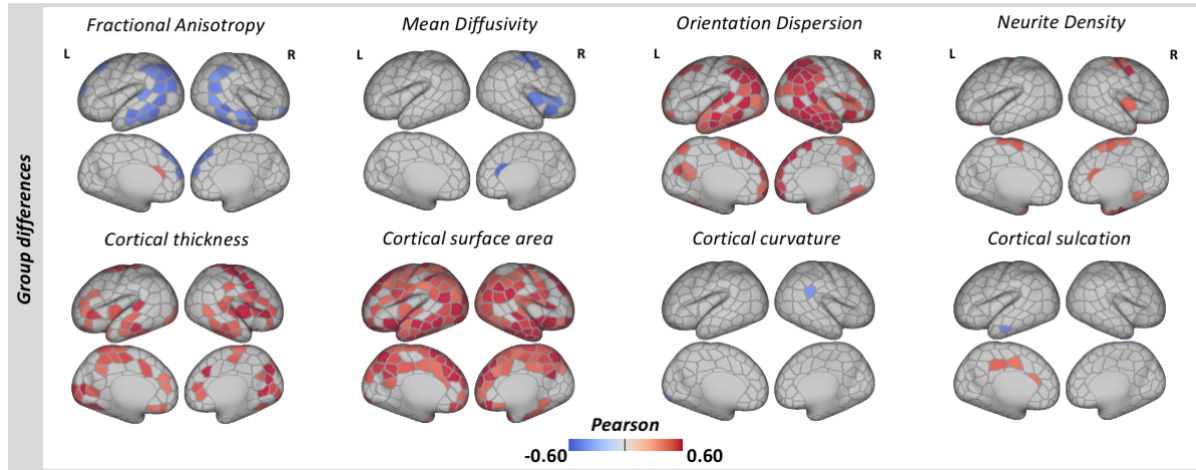
Supplementary Figure 5. Predicted versus observed age at scan (PMA) for the train and hold-out samples with best line of fit for the error-in-variables (EIV) hyperparameter optimised RF model.

RANDOM FOREST: 10% MOST IMPORTANT FEATURES FOR PREDICTING PMA AT SCAN



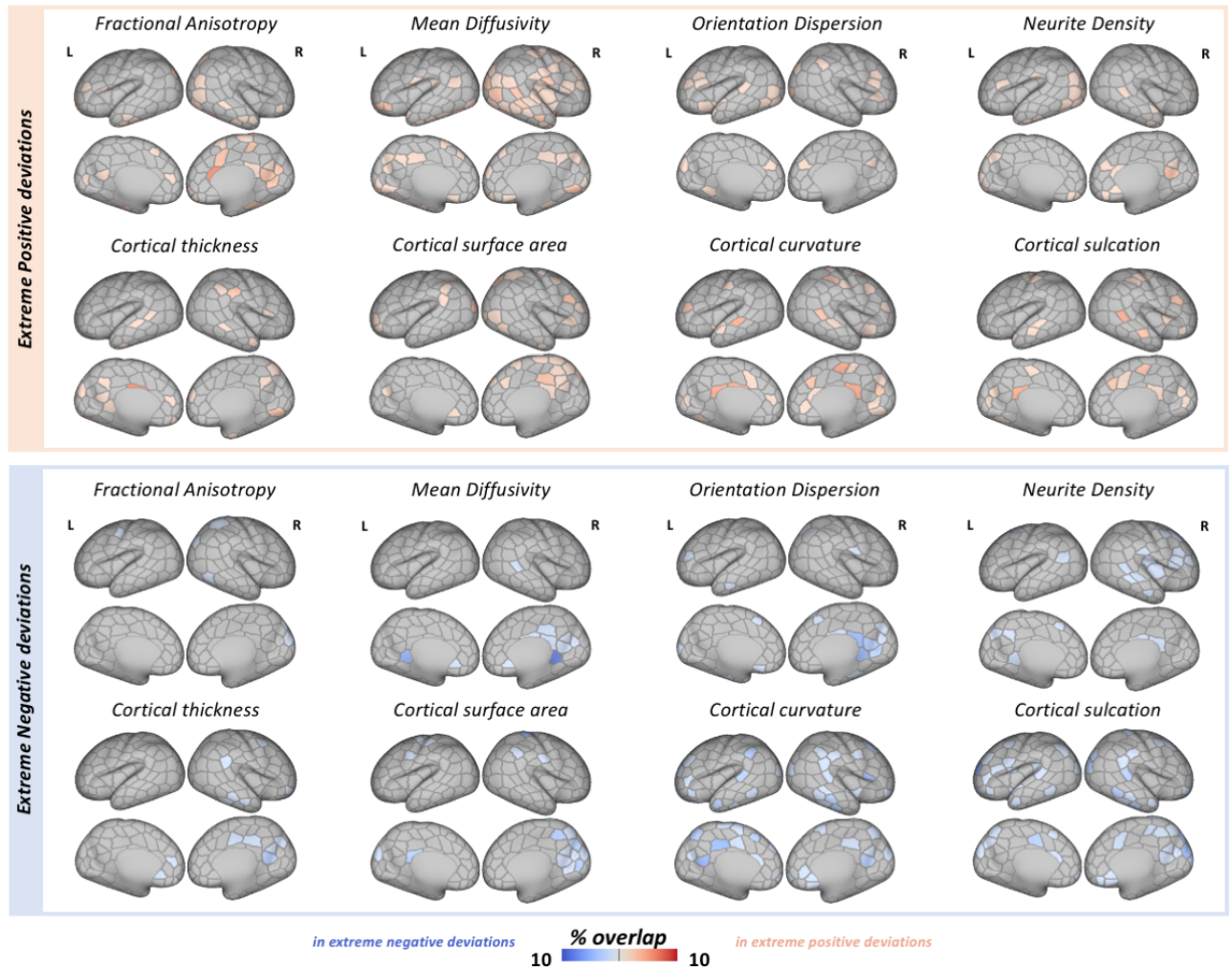
Supplementary Figure 6. Predicting PMA at scan using cortical surface features in term-born infants using RF regression. The 10% most important features (229) are shown.

CORRELATION WITH PMA AT SCAN IN THE PRETERM SAMPLE

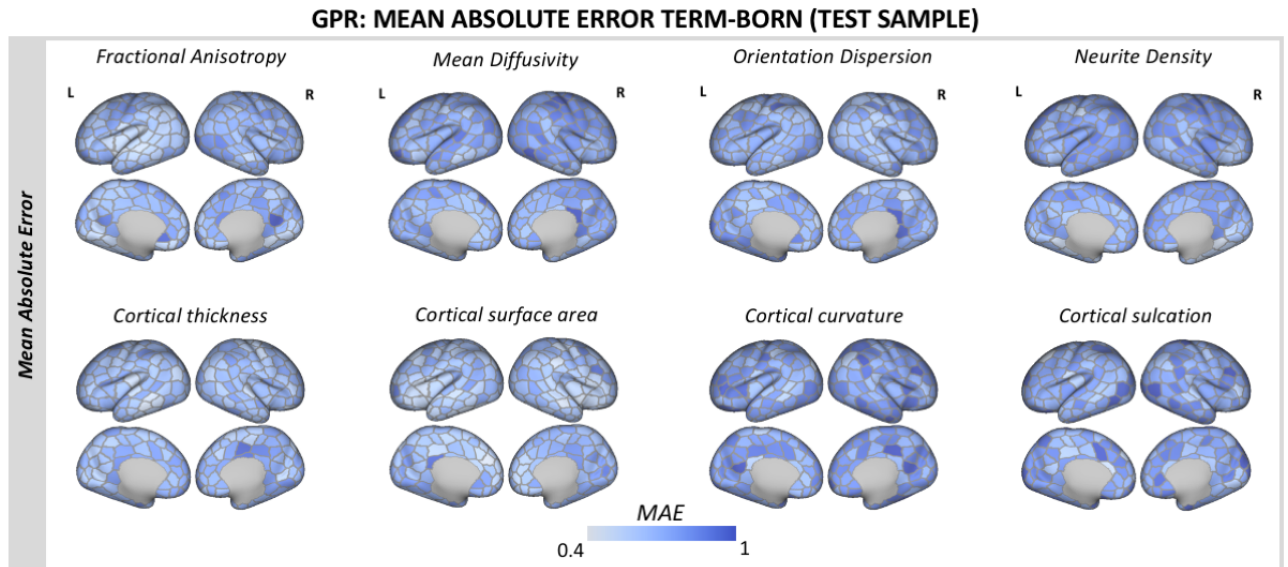


Supplementary Figure 7. Rapid regionally specific cortical micro- and macrostructure development in preterm infants at term-equivalent age. Pearson's correlation coefficients shown for all parcels indicating a significant ($p_{\text{mefwe}} < 0.05$) positive (red) or negative (blue) association with age (PMA at scan).

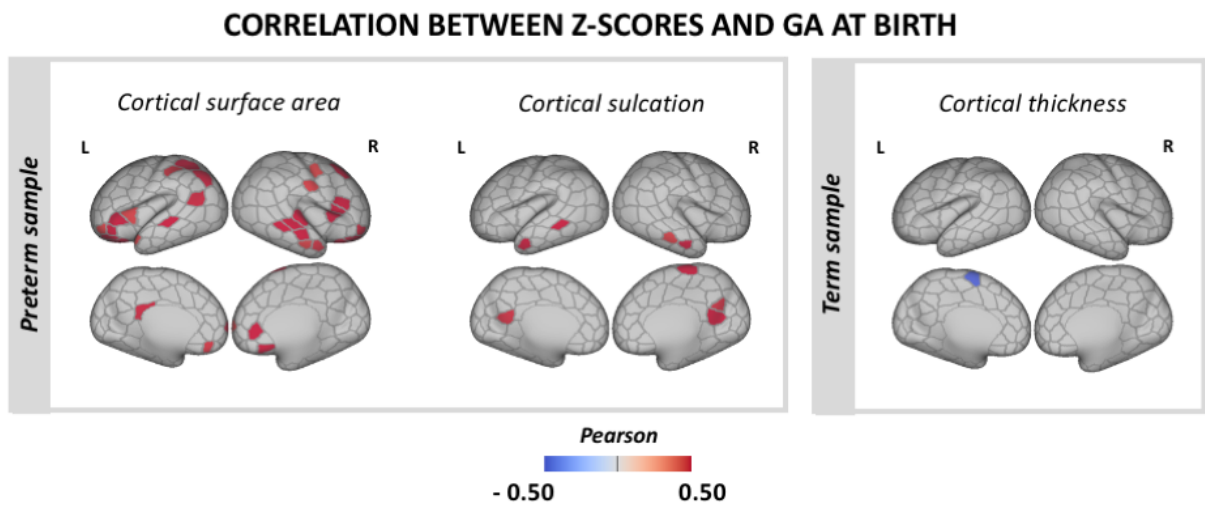
SPATIAL OVERLAP IN EXTREME DEVIATIONS FROM NORMATIVE DEVELOPMENT IN TERM INFANTS



Supplementary Figure 8. Spatial overlap in extreme positive/negative deviations from normative development in the hold-out test term-born sample. The overlap maps show the proportion of infants with extreme deviations ($Z > |3.1|$) from normative development for every parcel and cortical feature.



Supplementary Figure 9. Mean absolute error surface maps (in units of standard deviation) derived from the GPR for the hold-out term-born sample.



Supplementary Figure 10. Association between extreme deviations from normative cortical development and GA at birth. Pearson's correlation coefficients are shown for parcels indicating a significant ($p_{\text{mcfwe}} < 0.05$) positive (red) or negative (blue) correlation with GA at birth in the preterm and term-born samples separately.

Supplementary Tables:

Supplementary Table 1. Stages of quality control and exclusion criteria applied in sample size selection.

	Term	Preterm
Initial sample	400	109
sMRI T ₂ -weighted QC	-5	-2
dMRI QC score > 3.5	-23	-6
dMRI cropped cortex	-76	-10
dMRI to sMRI misalignment	-2	-5
Surface QC	-18	-10
Incidental findings (clinical sign.)	-17	*
Final Sample	259	76*

*One preterm infant had a gross clinical abnormality and was excluded from the group-wise analyses. This infant's data were kept in the individual GPR analyses.

References

- Christiaens D, Cordero-Grande L, Pietsch M, Hutter J, Price AN, Hughes EJ, Vecchiato K, Deprez M, Edwards AD, Hajnal J V, Tournier J-D. 2021. Scattered slice SHARD reconstruction for motion correction in multi-shell diffusion MRI. *Neuroimage*. 225:117437.
- Kirk TF, Coalson TS, Craig MS, Chappell MA. 2020. Toblerone: Surface-Based Partial Volume Estimation. *IEEE Trans Med Imaging*. 39:1501–1510.
- Makropoulos A, Robinson EC, Schuh A, Wright R, Fitzgibbon S, Bozek J, Counsell SJ, Steinweg J, Vecchiato K, Passerat-Palmbach J, Lenz G, Mortari F, Tenev T, Duff EP, Bastiani M, Cordero-Grande L, Hughes E, Tusor N, Tournier JD, Hutter J, Price AN, Teixeira RPAG, Murgasova M, Victor S, Kelly C, Rutherford MA, Smith SM, Edwards AD, Hajnal J V., Jenkinson M, Rueckert D. 2018. The developing human connectome project: A minimal processing pipeline for neonatal cortical surface reconstruction. *Neuroimage*. 173:88–112.